Nuclear Inst. and Methods in Physics Research, A 884 (2018) 18–24

Contents lists available at ScienceDirect

Nuclear Inst. and Methods in Physics Research, A

journal homepage: www.elsevier.com/locate/nima

A GEM-TPC in twin configuration for the Super-FRS tracking of heavy ions at FAIR

F. García [a,*], T. Grahn [a,b], J. Hoffmann [c], A. Jokinen [a,b], C. Kaya [c], J. Kunkel [c], S. Rinta-Antila [a,b], H. Risch [c], I. Rusanov [c], C.J. Schmidt [c], H. Simon [c], C. Simons [c], R. Turpeinen [a], B. Voss [c], J. Äystö [a,b], M. Winkler [c]

[a] Helsinki Institute of Physics, University of Helsinki, 00014 University of Helsinki, Finland
[b] Department of Physics, University of Jyväskylä, 40014 University of Jyväskylä, Finland
[c] GSI Helmholtzzentrum für Schwerionenforschung GmbH, Darmstadt 64291, Germany

ARTICLE INFO

Keywords:
Gas electron multiplier
Time projection chamber
Super-FRS
Tracking
Radioactive ion beam
Beam adjustment
FAIR
Fragment separator
GSI

ABSTRACT

The GEM-TPC described herein will be part of the standard beam-diagnostics equipment of the Super-FRS. This chamber will provide tracking information for particle identification at rates up to 1 MHz on an event-by-event basis. The key requirements of operation for these chambers are: close to 100% tracking efficiency under conditions of high counting rate, spatial resolution below 1 mm and a superb large dynamic range covering projectiles from $Z = 1$ up to $Z = 92$. The current prototype consists of two GEM-TPCs inside a single vessel, which are operating independently and have electrical drift fields in opposite directions. The *twin configuration* is done by flipping one of the GEM-TPCs on the middle plane with respect to the second one. In order to put this development in context, the evolution of previous prototypes will be described and its performances discussed. Finally, this chamber was tested at the University of Jyväskylä accelerator with proton projectiles and at GSI with Uranium, Xenon, fragments and Carbon beams. The results obtained have shown a position resolution between 120 to 300 μm at moderate counting rate under conditions of full tracking efficiency.

1. Introduction

The facility for antiproton and ion research (FAIR) [1,2], will provide an extensive range of beams; from protons, antiprotons to uranium at intensities up to 10^{11} particles/spill and with excellent beam quality in the longitudinal and transverse phase space.

The Superconducting Fragment Separator (Super-FRS) [3] is a powerful in-flight device which will provide spatially separated isotopic beams up to uranium projectiles. Its superiority to the present FRS [4] is the incorporation of more separation stages and larger aperture superconducting magnets. Due to the high-resolution achromatic mode of the Super-FRS, the tracking detectors are crucial to obtain precise momentum measurement of the fragments produced. These tracking devices can be used to apply position correction for the ion velocity whenever is needed. In addition, they are an inherent component to determine the corrections applied to energy loss (dE/dx) needed in the particle identification scheme of $\beta\rho$-TOF-ΔE.

The fragment separator (FRS), which is the predecessor of Super-FRS provides high energy and spatially separated monoisotopic beams of exotic nuclei of all elements up to uranium. At the present, the FRS uses conventional Time Projection Chambers (TPC) [5] for tracking. These chambers have a single proportional counter for amplification stage and induction of signals. They operate in P10 gas (Ar/CH_4 90/10) at 1 atm pressure, with a maximum counting rate capability of 100 kHz. By placing several TPCs downstream tracking for the experiments is currently done, however, it is possible only at a low rate.

The diagnostics for the Super-FRS will require tracking on an event by event basis, for beams extracted with spill length exceeding 100 ms of duration. The GEM-TPCs chambers together with Time of flight [6] detectors, Multi-Sample Ionization Chambers MUSIC [7] and Secondary Emission detectors (SEM grids) [8] will feed data to global NuSTAR event builder. Therefore, all data acquisition systems (DAQs) of these detectors should be integrated.

Furthermore, the requirements for the tracking detectors of the Super-FRS are:

- Close to 100% tracking efficiency at 1 MHz counting rate, given an overall hit density of 1 kHz/mm^2

* Corresponding author.
E-mail address: Francisco.Garcia@helsinki.fi (F. García).

https://doi.org/10.1016/j.nima.2017.11.088
Received 14 September 2017; Received in revised form 17 October 2017; Accepted 28 November 2017
Available online 7 December 2017
0168-9002/

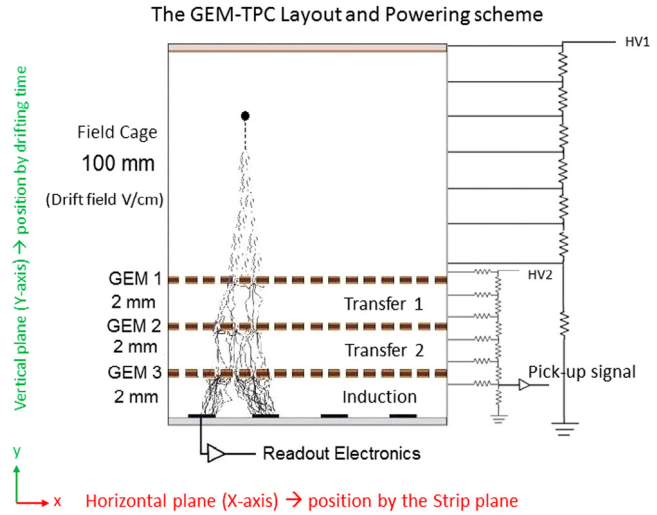

Fig. 1. The GEM-TPC layout. The main components: field cage, triple GEM stack, and the Front-end electronics. On the right side, the powering scheme.

- Spatial or position resolution of less than 1 mm
- Large dynamic range covering projectiles from Z = 1 up to Z = 92
- Minimal interference with the beam; low material budget and uniformity

The main function of these detection systems, distributed in diagnostics stations along the separator, is threefold: setting up and adjustment of the separator, providing means for machine safety monitoring and particle identification on an event-by-event basis.

One of the main challenges for all components of these detectors is to withstand the radiation damage produced by the primary projectiles and fragments, as for the background radiation. Hence long-term stability and resistance to aging are of paramount importance. Finally, the design of such detector systems should consider extensive operation periods without maintenance or external interventions, especially for those chambers located in the pre-separator.

Throughout this paper, the term *chamber* will be referred to the GEM-TPC as a whole and its functionalities however, *detector* will be used instead when a particular mechanism of its operation is discussed.

2. Principle of operation of the GEM-TPC

The layout of the GEM-TPC for tracking at the Super-FRS is shown in Fig. 1. The components of a GEM-TPC are field cage [9], GEM stack and front-end electronics. The GEM stack is used as an amplification stage and consists of three GEM foils [10] spaced by 2 mm each; forming two transfer gaps and one induction gap. With this last one located in between the third GEM foil and the anode strip plane.

The principle of operation is based on the generation of primary electrons in the working gas by traversing projectiles. Followed is the drift of these electrons, inside a very uniform electric field in the field cage, towards the anode strips. Upon arrival, signals will be induced e.g. in a similar way as for a typical Time Projection Chamber. However, the main difference resides on the amplification stage, which for the GEM-TPC [11] is done by a triple GEM stack. Which allows modulating the avalanche of electrons when needed i.e. the gain. Furthermore, it can be used to steer the space charge in the induction gap as well.

The powering scheme for the GEM-TPC is done by two independent high voltage power suppliers; HV1 provides bias voltage for the resistor divider of the field cage and HV2 for the triple GEM divider (See Fig. 1). By changing these two bias voltages, different regimes of operation can be set. Depending on the energy loss of the primary projectiles, the gain of a triple GEM stack needs to be varied, in order to make its detection possible. As an example, in previous experiments gain for protons was much higher than for Uranium beam due to differences in energy loss.

3. Experimental

3.1. GEM-TPC detector development

In an attempt to satisfy the requirements for tracking at Super-FRS, the concept of GEM-TPC was chosen. The first prototype was built by joining together a field cage from a conventional TPC already deployed along the FRS [12], developed by the Comenius University of Bratislava and a triple GEM stack as amplification stage.

The GEM foils for the stack were produced by CERN electronics workshop; however, the characterization and quality assurances (QA) was carried out by the Helsinki Institute of Physics. The protocols used for characterization and QA are well defined and developed during the production of the TOTEM triple GEM detectors for the LHC [13] and currently updated for the ALICE TPC upgrade [14].

After the integration the Helsinki–Bratislava prototype no. 1 [15] (HB1) was commissioned, and tested for the first time, at the FRS in 2010 with projectiles of ^{64}Ni at 550 MeV/u [16]. From the results good, spatial resolution in both coordinates was obtained. In addition, very stable operation throughout the whole experiment was observed. Despite these encouraging results, the overall counting rate was low reaching a maximum of 100 kHz under conditions of full tracking efficiency.

The spatial resolution obtained with HB1 was between 120 –300 μm in the horizontal plane and 125 μm on the vertical plane. The orientation of the chamber was such, that the position in the horizontal plane (X-axis) was given by the projection of the space charge on the readout strips (anode) and in the vertical plane (Y-axis) by the drift time of the electrons. However, the overall counting rate was limited by the use of delay lines for the readout.

In order to, increase the counting rate capability under conditions of full tracking efficiency, the GEM-TPC was equipped with high-density readout GEMEX [17,18] front-end cards. As a result of this integration process, two prototypes (Helsinki–Bratislava prototype no. 2 and no. 3 [19]) were assembled and commissioned. The main difference between them was the readout strip plane geometry as it is shown in Fig. 2.

For the HB2 the strips were in chevron configuration with a pitch of 3 mm and for HB3 parallel strips with a pitch of 0.5 mm. This last chamber had a density of readout channels four (4) times higher than HB2. A common feature between them was the cut-off of strips at the middle length, hence giving the possibility to have two detector-like sharing one single field cage.

After commissioning in the laboratory, the HB2 and HB3 were tested in 2012 at GSI. This time the primary beam projectiles were ^{197}Au with an energy of 750 MeV/u and intensity up to 10^7 ions/spill. The length of the spill was varied between 8–10 s with the beam illuminating the whole fiducial area. In addition, the beam geometry was focused and defocused. The spatial resolution obtained with both prototypes was very close to each other and in agreement with HB1, however this time at higher counting rate of 500 kHz at full tracking efficiency.

These prototypes gave us the opportunity to study several aspects; the impact of redundancy of readout channels and its tracking performance for different strip plane geometries. The conclusion was despite similar position resolution, HB2 was more sensitive to damaged or noisy channels, which resulted in partial loss of acceptance. Another aspect was the saturation of the readout channels, which was far more pronounced in HB2. This point out to the fact that, by splitting the cluster charge in many strips saturation of the channels is less critical. Especially for the case of readout electronics with small dynamic range.

3.2. GEM-TPC in twin configuration

From simulation results was found that none of the previous prototypes (HB1, HB2, and HB3) can achieve close to 100% tracking efficiency at 1 MHz counting rate [20], which is one of the requirements for the Super-FRS. Therefore, a new GEM-TPC design (see Fig. 3) was

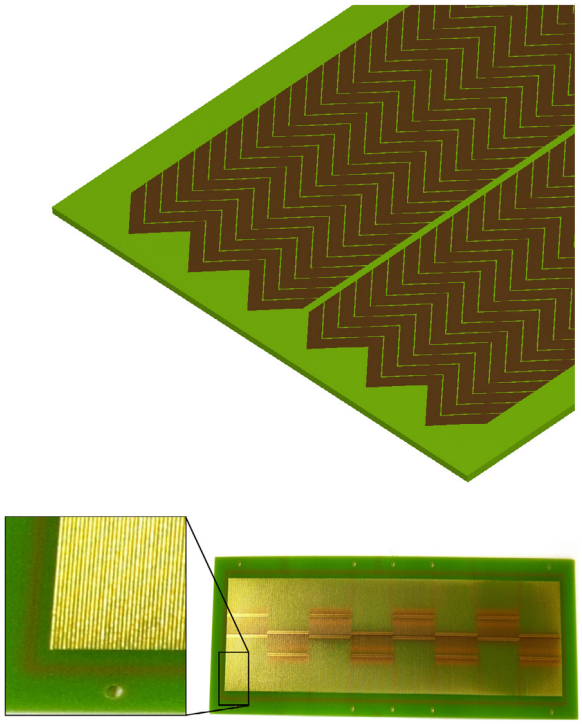

Fig. 2. Readout plane for the two GEM-TPC chambers; On top is the chevron strips of the HB2 and on the bottom, parallel strips for the HB3.

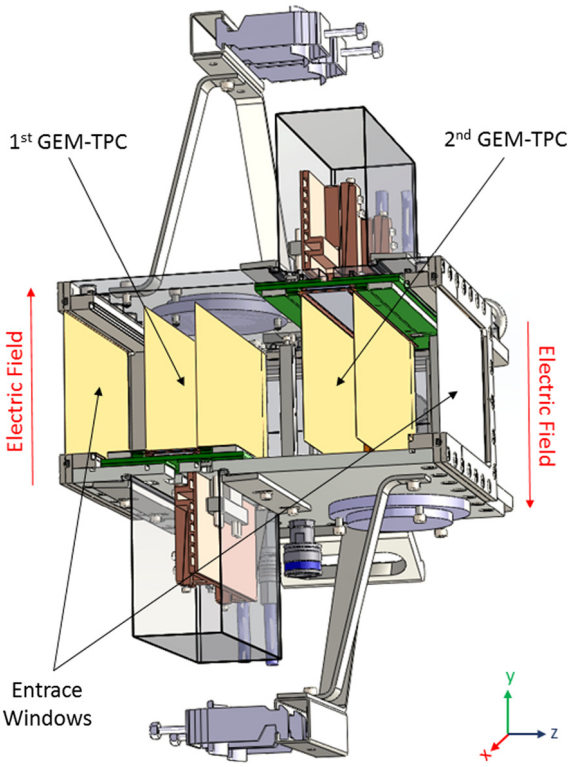

Fig. 3. Super-FRS GEM-TPC prototype HGB4 layout. It shows the two GEM-TPCs inside one vessel. In this configuration, the drift fields of the field cages are in opposite directions.

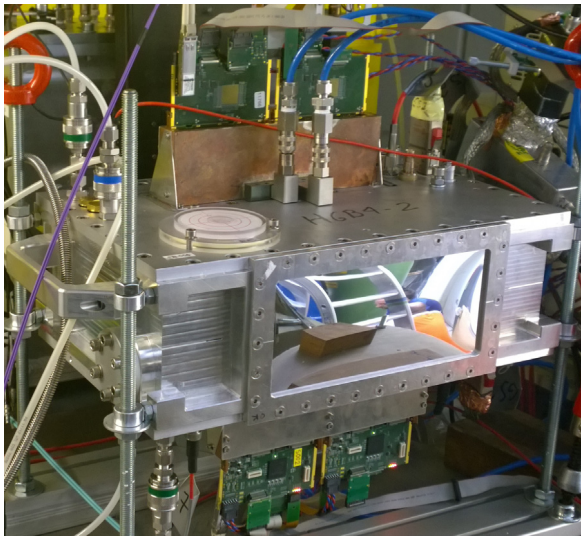

Fig. 4. Super-FRS GEM-TPC prototype HGB4, equipped with four front-end cards. On top, is the readout electronics for front GEM-TPC and on the bottom, is the back GEM-TPC respectively.

proposed, based on the concept of the TwinTPC [21]. Which consisted of adding two GEM-TPCs enclosed inside a single vessel. As a result, the prototype HGB4 (Helsinki–GSI–Bratislava prototype no. 4) was built.

This chamber has two GEM-TPCs inside a single vessel sharing same gas volume; with one of them flipped in the middle horizontal plane with respect to the second one. Hereby the notation of the HGB4 (GEM-TPC in twin configuration) will be first (1st) GEM-TPC for the one having the readout electronics on top and second (2nd) GEM-TPC for the one on the bottom.

In this configuration, the electric fields of the two field cages will be in opposite directions. Therefore, electrons generated by the ionization of the primary particles, are forced to drift in opposite directions e.g. in 1st GEM-TPC they will move towards the readout strip plane located on the top, and on the 2nd GEM-TPC to the bottom respectably. The signals induced on the anode strips of both GEM-TPCs will carry out information of charge and local time of arrival for each hit.

Related to the dimensions the HGB4 [22] chamber shown in Fig. 4 has an entrance window with a fiducial area of 22 x 10 cm^2. Thus, covering in the horizontal plane or X-axis 22 cm and in the vertical plane or Y-axis 10 cm. Furthermore, the traverse plane or Z-axis is 2.5 cm, which will be the thickness of gas seen by the primary projectile passing throughout the chamber.

The working gas used in all tests was P10 at 1 atm to allow direct comparison to the performance of conventional TPCs already deployed at the FRS as standard instrumentation. In addition, this gas has a suitable drift velocity and diffusion coefficients for this application. However, there are other types of gas mixtures that can be explored in the future as for instance: Ar/CO_2 (70/30), $Ar/CO_2/CF_4$ (45/15/40), etc.

4. Results of test beam campaigns

4.1. Simulations of energy loss

In order to, find detector working parameters e.g. bias voltages to the triple GEM divider and thus fix the intrinsic gain, simulations using GEANT4 [23] were performed. The results of energy deposition obtained for different projectiles is shown in Table 1. A cross-check for the energy deposition obtained by simulations was done and scales with Z^2, as expected [24].

From the Table 1 can be seen considerable variations of the energy deposited by projectiles, thus forcing to operate the detector at very different effective gains. For instance, throughout all the experiments and commissioning the effective gain was varied between 10 to 5000. An exception was for the case of Uranium beam, where a gain of 1 was used to avoid saturation of front-end electronics.

Table 1

Projectile (Energy)	GEM-TPC (Half)	**Energy deposited, MeV** (in 2.5 cm of P10 gas at 1 atm)	
		Mean	RMS
Protons	1st	$36.7\ 10^{-3}$	$3.3\ 10^{-3}$
(50 MeV)	2nd	$37.4\ 10^{-3}$	$3.1\ 10^{-3}$
^{12}C	1st	$240.2\ 10^{-3}$	$38.7\ 10^{-3}$
(660 MeV/u)	2nd	$241.4\ 10^{-3}$	$39.2\ 10^{-3}$
^{124}Xe	1st	20.1	$343.3\ 10^{-3}$
(660 MeV/u)	2nd	20.2	$349.6\ 10^{-3}$
^{238}U	1st	82.6	6.0
(300 MeV/u)	2nd	84.0	6.1

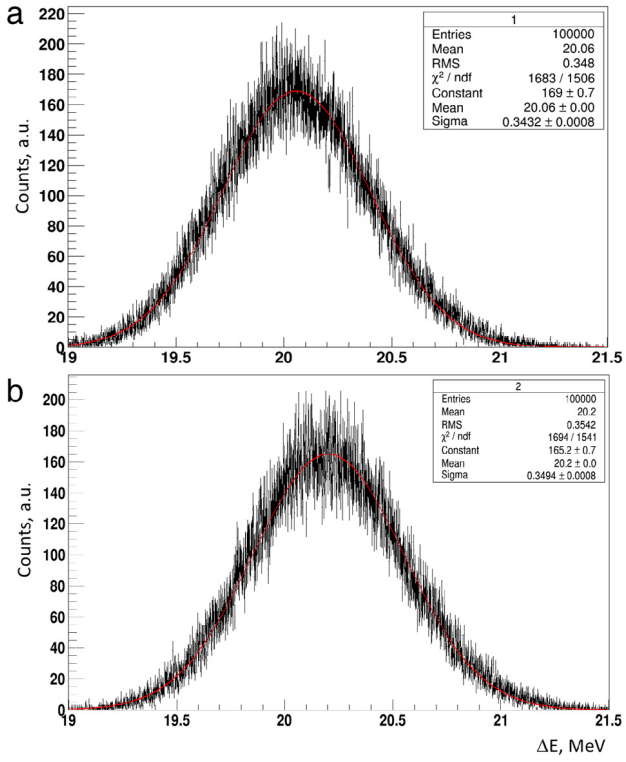

Fig. 5. Energy deposition distribution for ^{124}Xe beam projectiles simulations; in (a) for the 1st GEM-TPC and (b) for the 2nd GEM-TPC.

To illustrate the behavior of both GEM-TPCs when traversed by projectiles of^{124}Xe at 660 MeV/u, distributions of energy deposition obtained from simulations are shown in Fig. 5. For the 1st GEM-TPC the mean energy deposited was 20.06 MeV and for the 2nd GEM-TPC 20.20 MeV respectively. In this case downstream the primary ions will first hit the 1st GEM-TPC and then 2nd GEM-TPC

In fact, this was corroborated by the effective gain of both GEM-TPCs. When picking up signals from the bottom of the third GEM foil (See Fig. 1).

4.2. Experiments with heavy ions at GSI

The HGB4 was tested at GSI with^{238}U projectiles at 300 MeV/u,^{124}Xe and^{12}C at 660 MeV/u in two separated campaigns.

During 2014 campaign at GSI the HGB4 was located at CaveC. [25]. The geometry of the experiment is shown in Fig. 6. A plastic scintillator, marked as START, was located in front of a fission target and used for triggering (setting the starting time) of each event and downstream behind the ALADIN magnet HGB4 at a distance of few meters.

The observable for this measurement was the *Control Sum* (c.s.) and its RMS. In particular, these two parameters combined together are a figure of merit, of counting rate capability at full tracking efficiency.

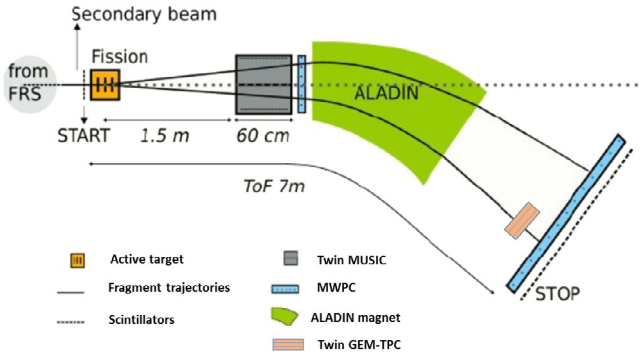

Fig. 6. The layout of the experimental setup for the testing of the Twin GEM-TPC (HGB4) in caveC. [25] during test beam in 2014.

Therefore, in ideal conditions the c.s. distribution will be a delta function with an infinite small RMS indicating full tracking efficiency can be achieved at very high counting rate. However, in reality, a Gaussian distribution is obtained and it is similar to the one shown in see Fig. 15. In fact, c.s. is the sum of drift time of electrons for both field cages related to starting time. The spread is the RMS, which is a convolution of many factors as for instance: contributions from longitudinal diffusion, which are related to the electric field strength, non-uniformities of the electric field, statistical fluctuations of the primary electrons and jitter contributions from readout electronics, etc. Results from simulations show, for the case of the time window of 1.6 μs (full drift time) and a cut-off of RMS of 21 ns the maximum counting rate achievable is 1.75 MHz at full tracking efficiency [20]. The equation for the c.s. is given by:

$$c.s. = T_{up} + T_{down} - 2T_{ref} \quad (1)$$

where: $T_{up} + T_{down}$ is the sum drift of the times for both field cages and T_{ref} is the reference time from the plastic scintillator.

In order to, measure the drift time for both GEM-TPCs in this experiment, the signals from the bottom of third GEM foil (GEM 3 bottom) were picked up (see Fig. 1) and pass to a constant fraction discriminator. Then, feed into multihit TDC (Caen V1290) and recorded. Then scan for different electric field strength was performed starting from 150 V/cm up to 320 V/cm [26]. Afterwards, the c.s. was calculated and a distribution was obtained.

The results from the c.s. scan obtained as a function of the electric field strength is shown in Fig. 7. On the abscissa is the value of the electric field, and the ordinate in the left side is the mean value of c.s. (in blue dots) and on the right side the RMS (in red). The RMS or sigma slightly changes for different electric field values, indicating the possibility to operate the chamber at lower bias voltages for the field cage. However, this was only observed for Uranium beams. For the case of protons, the RMS was much larger. One possible reason can be attributed to large impact ionization, which can smear out possible contributions to a jitter in c.s. coming from longitudinal diffusion. However, a detailed study will be needed to quantify this effect.

In another experiment carried out in 2016 at FRS, HGB4 was irradiated with a primary beam of^{124}Xe projectiles at 660 MeV/u and^{12}C at 660MeV/u.

The geometry of the setup consisted of a plastic scintillator, which was used for triggering and setting the starting time of each event. The scintillator was located right after beam pipe and in front of first TPC of the reference tracker. For this experiment, the HGB4 was placed in between two conventional TPCs in a DUT configuration.

In Fig. 8 is shown the schematics of the experimental setup. In addition, beam geometry was as in previous experiments focused and defocused illuminating the whole fiducial area. Related to the intensity the rates were varied from kHz/spill up to few MHz/spill.

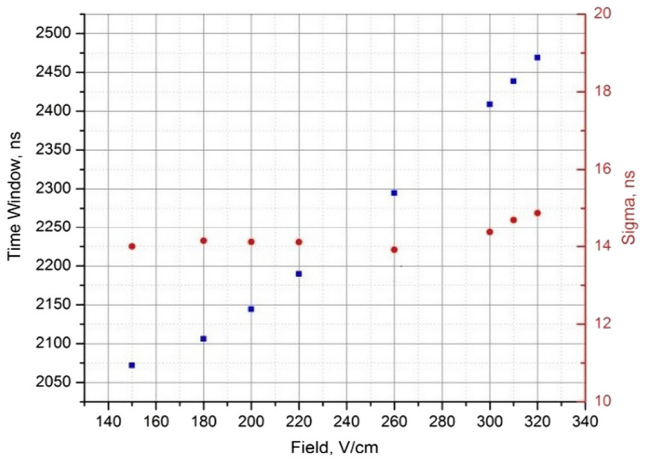

Fig. 7. The HGB4 *Control Sum* (blue dots) and its sigma (red dots). The time window is the total drift time taken by the electrons to drift across the full length of both field cages and the sigma is taken from this distribution at different field strengths [26].

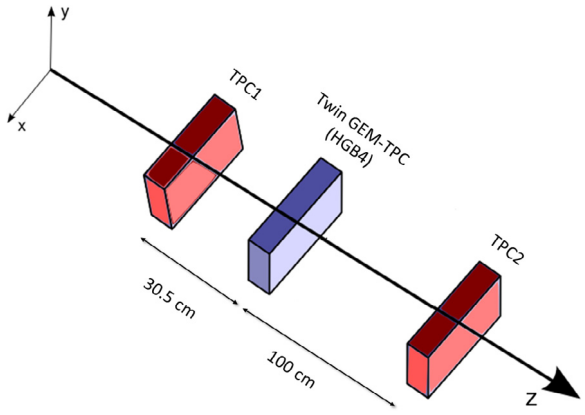

Fig. 8. Sketch of the experiment at GSI during the 2016 campaign. The HGB4 (Twin GEM-TPC) is located inside the reference tracker made of two conventional TPCs.

The new front-end cards GMX-NYXOR [27] were used for the readout of the two GEM-TPCs of HGB4. These front-end cards are a successor of GEMEX already used for HB2 and HB3. However, their main difference was done by physically separate; digital from the analogue part, i.e. placing them into two independent PCB boards. In fact, the GEMEX was split into two cards, in order to facilitate their modular debugging and testing. One GMX-NYXOR front-end card has two n-XYTER ASICs [28] and one n-XYTER can serve 128 strips. For reading out 512 strips of each GEM-TPCs, two cards are used, yielding a total of four (4) front-end cards for reading out the whole HGB4. In Fig. 9 the test stand of full readout chain for one GEM-TPC is shown.

From the data collected in one experiment of this campaign, correlation plot of hits projected on the horizontal plane (X-axis) of both GEM-TPCs was obtained. The correlation is shown in Fig. 10, on the abscissa, is the maximum amplitude taken from 1st GEM-TPC and corresponded hits from the 2nd on the ordinate respectively. It can be seen a good approximation of the hits' position for both GEM-TPCs, thus indicating tracking capability. However, the data used was only raw hits without any cuts or clusterization. Moreover, this information was accessible during the experiment by the online monitoring system.

In addition, was possible to resolve online single clusters too, as it is shown in Fig. 11.

A set of 9 (nine) consecutive clusters distributed along the horizontal plane (X-axis) for both GEM-TPCs was chosen. In the abscissa is strip number on the readout plane and in the ordinate amplitude in ADC counts.

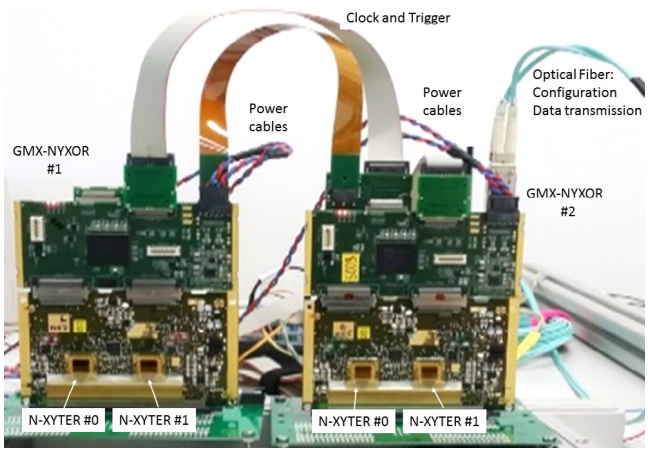

Fig. 9. The readout system GMX-NYXOR cards during testing in the laboratory.

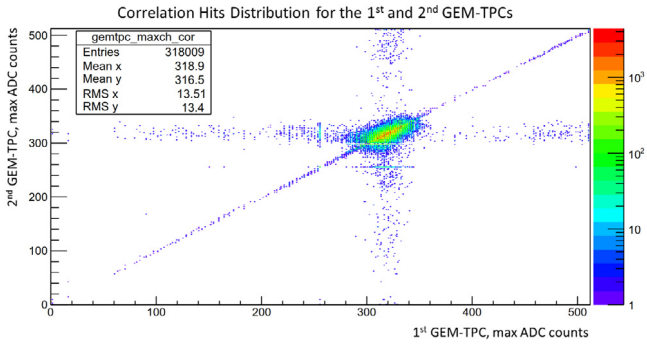

Fig. 10. Correlation of the signals Top and Bottom GEM-TPCs detectors of the HGB4 prototype, given for primary ^{124}Xe projectiles hitting the detector close to the central region.

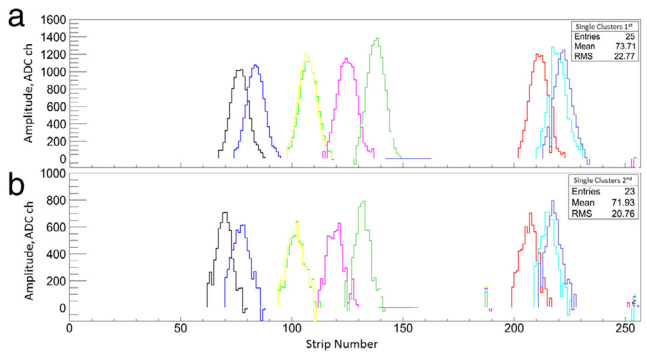

Fig. 11. Single clusters for primary ^{124}Xe @ 660 MeV/u beam projectiles. In (a) are the hits for the 1st *GEM-TPC* and on (b) are for the 2nd respectively. Most of the clusters involved for both GEM-TPCs have around 20 strips fired.

Furthermore, the clusters were color-coded, i.e. to allow direct comparison between them, because each one was generated by the same traversing projectile.

It can be seen that the quantity of strips fired inside a single cluster is nearly the same for both GEM-TPCs. However, differences can be seen in the trigger multiplicity plot. As for the hits' position all clusters were taken from raw data with no pedestal subtraction and no equalization, thus indicating a very uniform intrinsic gain of each GEM-TPC. By applying a Gaussian weighted fitting algorithm, the centroid of these clusters can be obtained, i.e. allowing to extract its position. A good

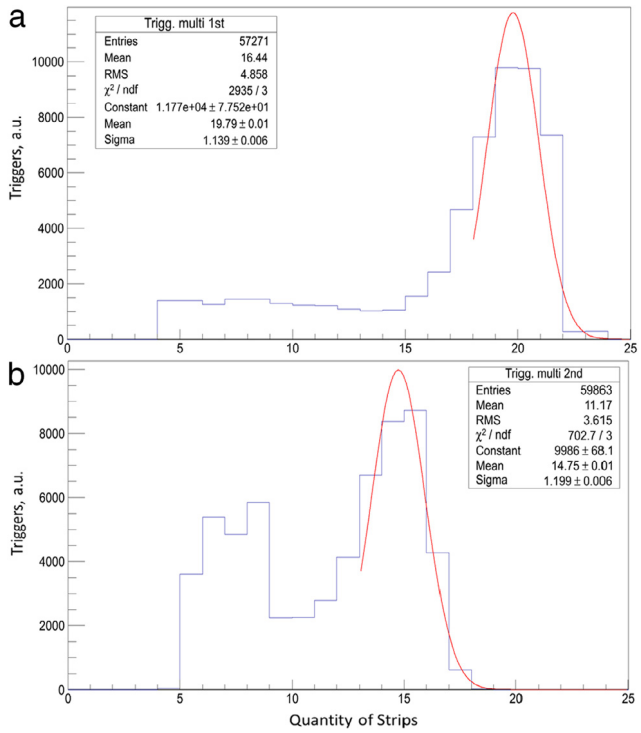

Fig. 12. Trigger multiplicity for ^{124}Xe beam projectiles; in (a) for the 1st GEM-TPC and in (b) for the 2nd GEM-TPC.

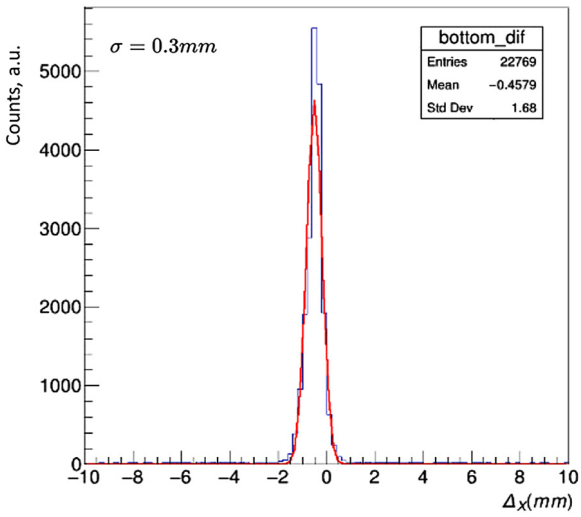

Fig. 13. Position resolution of HGB4 for incident ^{12}C beam projectiles for the horizontal plane (X-axis). The abscissa denotes the difference between the X coordinate extrapolated to the GEM-TPC position using the reference tracker and the one measured by HGB4.

Fig. 14. Analogue signals from the two GEM-TPCs of the HGB4 detector irradiated with protons at the 2.2. MHz rate; the upper part (in yellow) shows the signals from Top GEM-TPC and on the lower part (in red) the Bottom GEM-TPC respectively.

agreement in the position was found for all clusters. However, detailed analysis shows small systematically offset of 2 mm between them.

The cluster multiplicity shows how many strips are fired inside a single cluster. A crude calculation from online data shows that this parameter scales with the one obtained from Garfield simulations for same working gas [29] and drift length. Indicating a dominant contribution from transversal diffusion with small add effect from the triple GEM stack [30]. It is important to highlight that no clusterization algorithm has been yet implemented however, this work is in progress.

Instead, the trigger multiplicity will be shown. For better understanding, the differences between cluster and trigger multiplicities, this last one is obtained by summing up all channels (strips) fired in one trigger. However, the trigger multiplicity could be biased by noisy channels and multiple clusters inside a single trigger.

In Fig. 12 trigger multiplicity for^{124}Xe projectiles is shown. The quantity of strips fired in one trigger is shown in the abscissa and how many of them in the ordinate. The mean value of strips fired on both distributions is close to each other; with 19.79 strips for 1st GEM-TCP and 14.75 strips for 2nd respectively. It can be seen a low multiplicity tail on 2nd GEM-TPC, which can be attributed to noisy channels.

The method used to calculate the spatial resolution is based on computing the differences; between the extrapolated track position at the device under test (DUT), given by straight line from reference tracker and the position recorded by HGB4. These differences or residuals are collected for all tracks and forms a distribution. The RMS of this distribution will become the spatial resolution. In Fig. 13 the spatial or position resolution is shown and the value obtained was 300 µm. This resolution was found to be twofold: close to the one obtained with all previous prototypes (HB1, HB2, HB3) and well below the required limit.

In summary, HGB4 has performed as expected with no major incidents registered during the whole campaign. In addition, HGB4 worked for long extended periods at high counting rate (over 1 MHz) showing remarkable long-term stability. Under these conditions, it was possible to acquire large amounts of data, mainly by carrying out multiparameter scans as for instance GEM stack gain, electric field variations on the field cage versus beam intensity.

4.3. Experiments with protons at Jyväskylä

Testing GEM-TPC sensitivity for protons was one of the most important experiments for the GEM-TPC concept since it was not possible to be done with conventional TPCs currently operating at FRS. Therefore, a test program was proposed at the University of Jyväskylä accelerator facility with proton projectiles at 50 MeV/u. This test was used to provides information on the long-term operation stability of HGB4 under conditions similar to the Super-FRS.

The geometry of the experiment was very close to the one in Fig. 8, however for this test no reference tracker was present. This was mainly due to the low kinetic energy of the protons.

Instead, a plastic scintillator was located downstream and in front of HGB4. From data collected, a c.s. was obtained in conditions of the high-intensity proton beam. The particle rate was varied from 1 kHz up to 7 MHz in the full acceptance.

Signals recorded by an oscilloscope at a particle rate of 2.2 MHz are shown in Fig. 14. On the two-color plot, the raw signals from 1st GEM-TPC are in yellow and from 2nd in red respectively. The maximum achievable counting rate during this test was 7.9 MHz i.e. 7.9 times

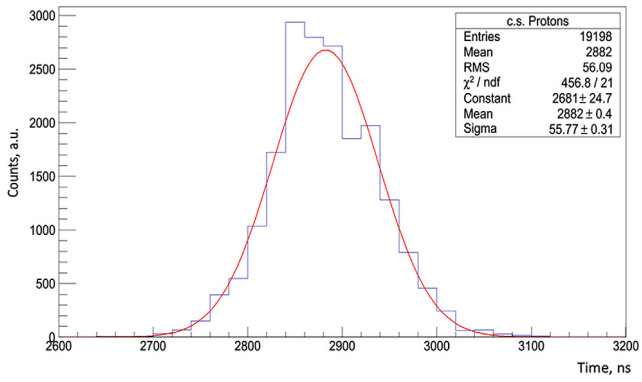

Fig. 15. Control Sum measured for protons at 50 MeV/u energy and a rate of 750 kHz traversing perpendicularly the HGB4. This drift field strength was 290 V/cm.

higher than the actual counting rate at the Super-FRS. In a similar way, like in previous experiments with heavy ions, multiparameter scans were performed.

From the signals obtained two characteristics can be highlighted; correlation of hits position in time for both GEM-TPCs, whilst differences in effective gain are clearly seen. The magnitude of this difference was of 2 and the reason was found later; to be a malfunctioning electrical contact on the GEM stack of 2nd GEM-TPC. The bad electrical contact on the bottom flap reduced the voltage drop across the third GEM foil, thus producing lower gain.

The c.s. measured for protons at 50 MeV/u is shown in Fig. 15. A single Gaussian describes the data and no shoulders or any structure within this distribution is observed. The RMS extracted is 55.77 ns, which is a factor of 3.9 higher than for Uranium projectiles (Fig. 7). For this analysis, only 25% of triggers were used due to the small acceptance of the trigger scintillator. Nevertheless, the chamber was fully illuminated during these tests.

Possible reasons behind broadening of c.s. can be attributed to the scattering of the protons in Air before entering to HGB4 or the rescattering in the scintillator and finally statistical fluctuation of the primary electrons generated in the impact ionization. In addition, the longitudinal diffusion was a contributing factor found when comparing the c.s. taken for two different electric fields. As it was mentioned before for this experiment there was no reference tracker, therefore no preselection of tracks based on the incident angle could be done.

In summary, the experiment with irradiation of protons demonstrates two main things: the first one is the sensitivity of HGB4 to light ions at full tracking efficiency. The second was good long-term stability under conditions of a high-intensity beam.

However, optimizations are still needed, in order to optimize the timing performance. Currently, there are ongoing activities to optimize the GEM stack divider for P10 gas and tests with protons are foreseen at the end of 2017.

5. Conclusions

- The GEM-TPC has been developed and will be used as standard instrumentation for tracking at the Super-FRS.
- The GEM-TPC was tested in several beam campaigns with projectiles of: ^{238}U, ^{197}Au, ^{124}Xe, ^{64}Ni, ^{12}C and protons.
- The position resolution achieved in the horizontal plane (X-axis) was between 120 μm and 300 μm and for the vertical plane (Y-axis) of 125 μm.
- There are indications that the intrinsic rate capability is well above the required limit of 1 MHz. Studies of tracking efficiency and spatial resolution as a function of the rate will be available soon.

Acknowledgments

Acknowledgments to colleagues of the FRS team: C. Caesar, H. Heggen, N. Kurz, C. Nociforo and A. Prochazka at GSI for the extensive support during the test beam campaigns. Many thanks to the accelerator team at University of Jyväskylä and special thanks to A. Virtanen and H. Kettunen. At CERN special thanks to R. de Oliveira for the production of GEM foils. At HIP many thanks to J. Heino for helping during QA and framing. Thanks to S. Petri for the organization of the experiment at caveC.

References

[1] Conceptual design report (CDR) and Baseline technical report (BTR) for FAIR at http://www.gsi.de/fair/reports/index.htmln.
[2] G. Rosner, Future facility: FAIR at GSI, Nucl. Phy. B (Proc. Suppl.) 167 (2007) 77.
[3] H. Geissel, et al., The Super-FRS project at GSI, Nucl. Instr. and Meth. in Phys. Res. B 204 (2003) 71.
[4] H. Geissel, et al., The GSI projectile fragment separator (FRS): A versatile magnetic system for relativistic heavy ions, Nucl. Instr. and Meth. B 70 (1992) 247.
[5] R. Janik, et al., Time projection chambers for tracking and identification of radioactive beams, Nucl. Instr. and Meth. A 419 (1998) 503.
[6] O. Kiselev, et al., Radiation hardness test o fSi detectors for time of flight measurements at the super-FRS, MU-NUSTAR-FRS-03. GSI Scientific report 2014, 2014, 137 p.
[7] J.L. Rodríguez-Sanchez, et al., Phys. Rev. C 90 (2014) 064606.
[8] C. Nociforo, et al., Profile monitors for the super-FRS, FG-SFRS-03. GSI scientific report 2014, 2014, 499 p.
[9] R. Janik, et al., TPC cathode read-out with C-pads, Nucl. Instr. and Meth. A 598 (2009) 681.
[10] F. Sauli, GEM: A new concept for electron amplification in gas detectors, Nucl. Instrum. Methods A 386 (1997) 531–534.
[11] B. Ketzer, B. Voss, F. Garcia, et al., A large ungated TPC with GEM amplification, Nucl. Instr. and Meth. A 869 (2017) 180.
[12] R. Janik, et al., Time projection chamber with C-pads for heavy ions tracking, Nucl. Instr. and Meth. A 640 (2011) 54.
[13] M. Quinto, et al., The TOTEM GEM telescope (T2) at the LHC, Nuclear Phys. B 215 (2011) 225–227.
[14] H. Appelshaeuser, C. Lippmaan, F. Garcia, et al., Upgrade of the ALICE Time Projection Chamber TDR CERN-LHCC-2013-020; ALICE-TDR-016, 2013.
[15] F. Garcia, et al., IEEE Nuclear Science Symposium conference record, ISSN: 1095-7863, 2009, pp. 269–272.
[16] F. Garcia, et al., IEEE Nuclear Science Symposium conference record, ISSN: 1082-3654, 2011, pp. 1788–1792.
[17] J. Hoffmann, et al., GEM-TPC Data Acquisition System Development GSI Report 2011/2012, 2012, 255 p.
[18] B. Voss, et al., GEMEX, a compact readout system. 2012. IEEE Nuclear Science Symposium conference record, 2012, pp. 678–679.
[19] F. Garcia, et al., IEEE Nuclear Science Symposium conference record, ISSN: 1082-3654, 2012, pp. 1119–1123.
[20] F. Garcia, et al., Super-FRS GEM-TPC Development for the FAIR facility Status Report presentation. NUSTAR meeting at Helsinki, 2013.
[21] B. Sitar, et al., In-Beam Test of the TwinTPC at FRS. FG-SFRS-04, GSI Scientific report 2014, 2014, 500 p.
[22] F. Garcia, et al., talk at the 3rd Conference on Micro-Pattern Gaseous Detectors and 11th RD51 Collaboration Meeting, Zaragoza, Spain, 2013.
[23] J. Allison, et al., Geant4 – a simulation toolkit, Nucl. Instr. and Meth. A 506 (2003) 250.
[24] B.A. Weaver, A.J. Westphal, Energy loss of relativistic heavy ions in matter, Nucl. Instr. and Meth. B 187 (2002) 285.
[25] L. Audouin, et al., Nuclear Physics and Gamma-Ray Sources for Nuclear Security and Nonproliferation procedings. Ricotti, Tokai-mura, Japan 28–30 January 2014.
[26] F. Garcia, et al., Twin GEM-TPC Prototype (HGB4) Beam Test at GSI – A Development for the Super-FRS at FAIR. GSI Report 2014/2015-1, 2015, 140 p.
[27] Private communications from N. Kurtz and H. Heggen.
[28] C.J. Schmidt, et al., The n-XYTER Reference Manual. Chip version 1.0.
[29] A. Prochazka, et al., Simulations of the GEM-TPC response. GSI-SR2013-FG-S-FRS-12, GSI Report 2014-1.
[30] E. Oliveri, The forward inelastic telescope T2 for the TOTEM experiment at the LHC (Ph.D. thesis). CERN-THESIS-2010-178, 2010.